J Radioanal Nucl Chem (2010) 283:713–718
DOI 10.1007/s10967-009-0401-3

Determination of naturally occurring radionuclides in selected rocks from Hetaunda area, central Nepal

Gabriela Wallova · Kamala Kant Acharya · Gabriele Wallner

Received: 23 October 2009 / Published online: 3 December 2009

Abstract The specific activities of the naturally occurring radionuclides ^{238}U, ^{232}Th, and ^{40}K were measured in rock samples from the Hetaunda area, central Nepal, using gamma spectrometry. The specific activities were found to be in the range of 17–95 Bq kg^{-1} for ^{238}U, 24–260 Bq kg^{-1} for ^{232}Th and 32–541 Bq kg^{-1} for ^{40}K. From these data absorbed dose rates in air and annual effective doses were calculated and compared with respective data from the UNSCEAR compilation. The results from our study open the door to the safe applicability of most of the investigated materials as a cheep building material.

Keywords Uranium, thorium and ^{40}K activity concentrations · Rock samples · Gamma spectrometry · Dose calculation · Nepal

Introduction

The radionuclides occurring in our environment can be divided into (i) those formed from cosmic radiation, (ii) those with lifetimes comparable to the age of the earth, (iii) those that are part of the natural decay chains beginning with thorium (^{232}Th) and uranium isotopes (^{238}U and ^{235}U), and (iv) those introduced into nature by modern techniques. The respective sources can be categorized as: (i) cosmogenic, (ii) and (iii) primordial, and (iv) anthropogenic [1].

One of the main sources of human radiation exposure is the radioactivity of the soil and the underlying bed-rock. Usually more than 50% of our annual effective radiation dose comes from inhalation of the ^{238}U decay progeny ^{222}Rn and its daughters, and about 10% derives from intake of radionuclides via ingestion of water and food stuff. External terrestrial radiation sources contributing also around 10% of the annual dose are mainly ^{40}K and the γ-emitting decay products of ^{238}U and ^{232}Th. Thus, the knowledge of the distribution of these radionuclides is of principal importance [2–12].

In this paper we measured the specific activities of the naturally occurring radionuclides ^{238}U, ^{232}Th and ^{40}K in rock samples obtained from the Hetaunda area, central Nepal. From these data we calculated the absorbed dose rates in air at a level of 1 m above ground and made estimations of the annual effective dose to people due to outdoors engagement by using the occupancy factor and the conversion coefficient given by UNSCEAR [13]. Also the indoor annual effective dose to people living in a house built of the respective rock material was calculated. These results are of general interest since such rocks are often used as building and ornamental materials.

Experimental

Sampling

The study area lies in the Central Nepal Himalaya between latitudes and longitudes around 27°30′ north and 85°04′ east (Fig. 1). Politically this area lies in the Makawanpur district of Narayani Zone (Hetaunda Area). Geologically

G. Wallova (✉) · G. Wallner
Institut für Anorganische Chemie, Universität Wien, Währinger Str. 42, 1090 Vienna, Austria
e-mail: gabriela.wallova@univie.ac.at

K. K. Acharya
Central Department of Geology, Tribhuvan University, Kirtipur, Nepal

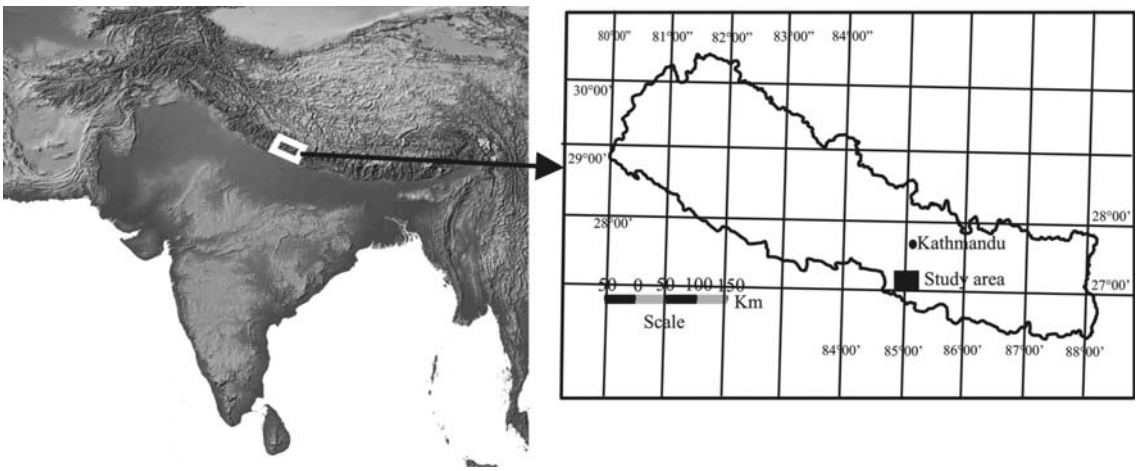

Fig. 1 Location map of the study area

the area comprises three successions of rock namely: The Siwalik, the Nawakot Complex (Lesser Himalaya) and the Kathmandu Complex (Higher Himalaya). Starting from the south, the first sample (code 64) was taken from the Benighat Slate of the Nawakot Complex. This unit mainly consists of graphitic slate with few bands of carbonate rocks named as Jhiku Carbonate. The next three samples (71, 70, and 69) stem from the Robang Formation mainly consisting of phyllites. The Main Central Thrust (MCT) brings the high grade rocks of the Raduwa Formation and the Bhainsedobhan Marble (sample 68) belonging to the Kathmandu Complex above the Robang Formation of the Nawakot Complex. The last sample (code 66) was taken from the Kalitar Formation of the Kathmandu Complex built up mainly by mica schist. The name of these formations was adopted after Stöcklin and Bhattarai [14]. All sampling sites lie between 400 and 1,100 m a.s.l. north of the Main Boundary Thrust (MBT) and in the vicinity of the MCT (see also geological map and cross-section in Fig. 2).

The collected samples were cleaned by removing the outer weathered layer, grinded, sealed in plastic Marinelli beakers and stored for 1 month before measurement in order to achieve complete ingrowth of ^{222}Rn together with its daughter products (the ^{220}Rn daughters are in radioactive equilibrium already after 2 days).

Gamma spectrometry and calculations

The activity concentrations of the primordial radionuclides ^{40}K, ^{238}U and ^{232}Th in grinded rock samples were determined using a Reverse Electrode Ge Detector (Canberra GR 2020) with 20% efficiency relative to NaI and 3 keV resolution. The detector calibration was verified with the standard reference sample IAEA-135 (radionuclides in Irish Sea sediment) measured in the same counting geometry as used for the samples of interest. Samples were counted for 17 h, while the counting time for the background was 60 h.

While the ^{40}K activity was measured directly (peak energy 1,460.8 keV, 10.7%), ^{238}U and ^{232}Th were evaluated indirectly via daughter products: ^{226}Ra (186 keV, 3.28%), ^{214}Pb (352 keV, 37.1%) and ^{214}Bi (609 keV, 46.1%) for ^{238}U determination, ^{228}Ac (911 keV, 29%), ^{212}Pb (239 keV, 43.1%) and ^{208}Tl (583 keV, 86%, branching ratio 36.2%) for ^{232}Th determination [2].

The specific activity A_i (in Bq kg^{-1}) of a nuclide i, is given by:

$$A_i = \frac{N_{Ei}}{\varepsilon_E \times t \times \gamma_{Ei} \times M_s},$$

where N_{Ei} is the netto peak area of a peak at energy E originating from a decay of nuclide i, ε_E is the detection efficiency at energy E, t is the counting time in seconds, γ_{Ei} is the decay probability of nuclide i via the measured transition at energy E, and M_s is the sample mass in kg.

From these specific activities A_i, elemental concentrations F_E of thorium, uranium, and ^{40}K were calculated by the formula:

$$F_E = \frac{M_N C}{\lambda_N \times N_A \times f_N} \times \frac{1}{n} \times \sum_n A_i,$$

where F_E is the fraction of element E (K, U or Th) in the sample (in % or ppm), M_N and λ_N is the atomic mass (kg mol^{-1}) and the decay constant (s^{-1}) of the respective parent radionuclide (^{40}K, ^{238}U or ^{232}Th) and f_N is the fractional atomic abundance of ^{40}K, ^{238}U or ^{232}Th in natural samples, N_A is Avogadro's number (6.023×10^{23} atoms mol^{-1}), C is a constant (with a value of 100 or 1,000,000) that converts the ratio of the element mass to soil mass into a percentage and ppm, respectively, and A_i is the specific activity of ^{40}K ($n = 1$) or that of the above given daughter nuclides in the decay series of ^{232}Th ($n = 3$) and ^{238}U

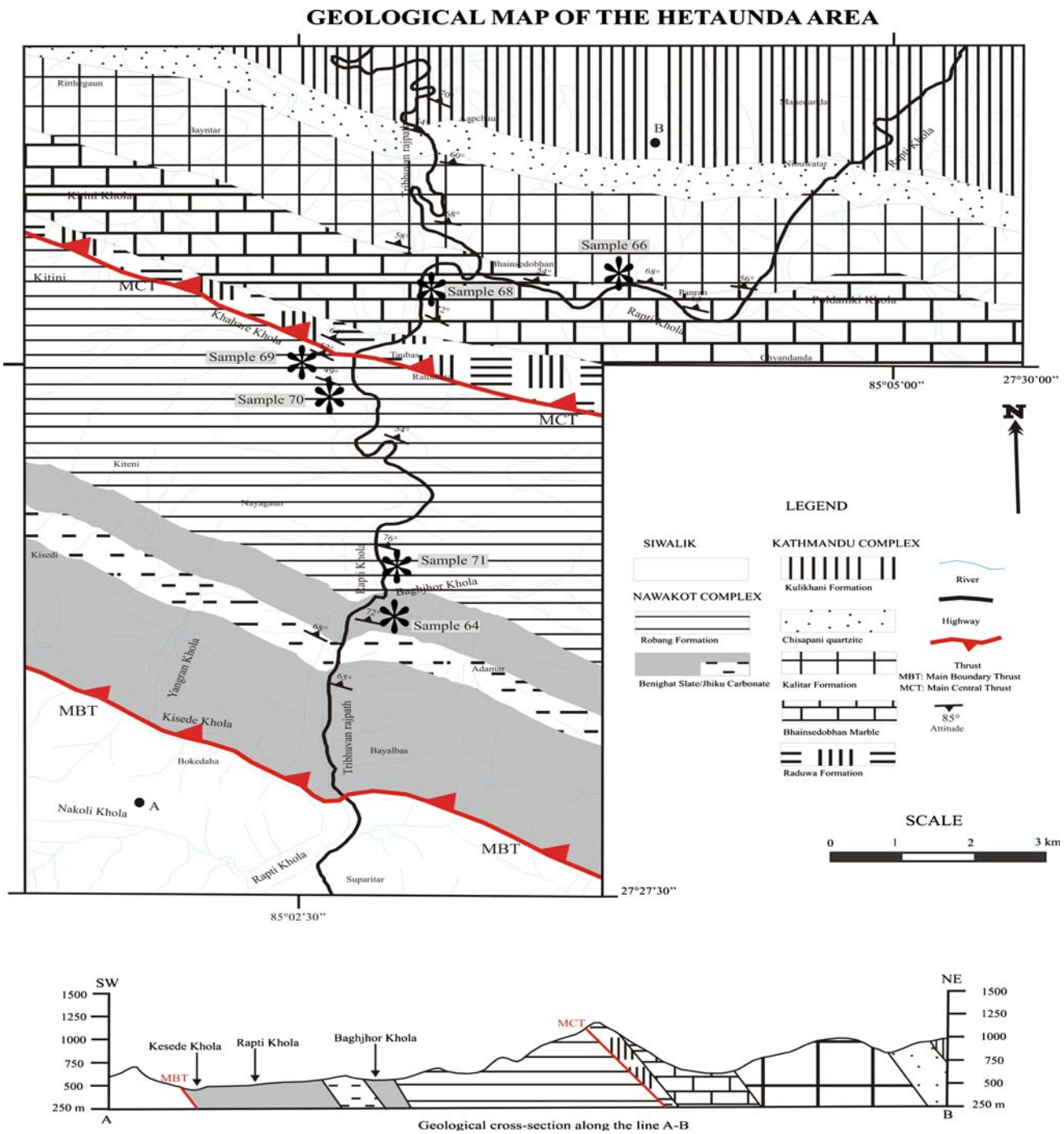

Fig. 2 Geological map and cross-section of the study area

($n = 3$). Total elemental concentrations are reported in units of parts per million (ppm) for thorium and uranium, and in percent (%) for potassium [3–5].

The absorbed dose rates in air at about 1 m above ground due to the terrestrial gamma radiation were calculated using the following equation [15, 16]:

$$D\ (\text{nGy h}^{-1}) = 0.043C_{^{40}\text{K}} + 0.662C_{^{232}\text{Th}} + 0.427C_{^{238}\text{U}}$$

$C_{^{40}\text{K}}$, $C_{^{232}\text{Th}}$, and $C_{^{236}\text{U}}$ are the respective specific activities in Bq kg^{-1}, and 0.043, 0.662 and 0.427 are the corresponding dose conversion factors in nGy h^{-1} per Bq kg^{-1}.

The annual effective dose rates H_E from outdoor exposition (in mSv/a) were calculated as follows:

$$H_E = D \times T \times F,$$

where D is the calculated dose rate (nGy h^{-1}), T is the outdoor occupancy time (0.2 × 24 h × 365.25 days) and F is the conversion factor (0.7 Sv Gy^{-1}) [13, 17].

Results and discussion

Table 1 summarizes the specific activities of ^{226}Ra, ^{214}Pb and ^{214}Bi (^{238}U daughter products) as well as of ^{228}Ac, ^{212}Pb and ^{208}Tl (^{232}Th daughter products), obtained by γ-spectrometry of our samples together with their corresponding 1σ-uncertainties. In the decay chains both ^{226}Ra and ^{228}Ac are precursors of the respective radon isotopes, while the other investigated nuclides are radon daughters. The good correspondence between precursor and daughter values shows that radon could not escape from our samples during measurement and confirms the reliability of our data. In order to make the comparing of the ^{232}Th daughter results more convenient, the real ^{208}Tl activity was divided by the branching ratio 0.362 and given in quotation marks as "^{208}Tl". Table 2 gives the specific activities of ^{238}U and ^{232}Th calculated from the data given in Table 1 as well as the specific ^{40}K activity of the investigated rock samples. These values were converted to elemental concentrations given in ppm uranium and thorium, and % potassium in Table 3.

As in soil samples, also in most of these rock samples ^{40}K exhibited a specific activity one order of magnitude higher than that of ^{238}U and ^{232}Th. The specific activities were found in the range of 17–95 Bq kg^{-1} for ^{238}U, 24–260 Bq kg^{-1} for ^{232}Th and 32–541 Bq kg^{-1} for ^{40}K.

These values will now be compared with data from UNSCEAR[13], giving median values from reported radionuclide surveys from all over the world. While the UNSCEAR values are 35, 30 and 400 Bq kg^{-1} for ^{238}U, ^{232}Th and ^{40}K, respectively, 4 of our investigated rock samples showed radioactivity levels clearly higher than the cited median levels. Concerning ^{40}K, three samples were only slightly higher than the median, concerning ^{238}U and ^{232}Th, 2 and 3 samples were higher than the median level by at least a factor of 2. Striking was the high ^{232}Th level in the sample Granite Schist 66 (260 Bq kg^{-1}), being an order of magnitude in excess of the median (this sample showed also the highest ^{238}U concentration: 95 Bq kg^{-1}).

In Table 4 the absorbed dose rates in air at a level of 1 m above ground are summarized. Although we investigated only a limited number of samples, we suppose the order of magnitude of our values to be representative due to the fact, that the selected rock types are predominant in the respective sampling areas. With the exception of the marble and the amphibolite samples (29 and 35 nGy h^{-1}, respectively), all calculated dose rates were higher than 90 nGy h^{-1}, with a maximum dose rate of 228 nGy h^{-1} (Granite Schist 66). UNSCEAR[13] summarized countries with results less than 40 nGy h^{-1} as "countries with the lowest values", while "countries with the highest values"

Table 2 Activity concentrations of ^{238}U, ^{232}Th and ^{40}K in the investigated samples

Rock type	Specific activity (Bq kg^{-1}) ± 1σ-uncertainties		
	^{238}U	^{232}Th	^{40}K
Granite Schist 66	95 ± 3	260 ± 5	359 ± 18
Marble 68	17 ± 1	24 ± 3	136 ± 15
Phyllite 69	40 ± 2	94 ± 3	541 ± 22
Amphibolite 70	21 ± 2	38 ± 2	32 ± 3
Phyllite 71	43 ± 2	89 ± 4	412 ± 21
Graphite Slate 64	86 ± 3	57 ± 3	430 ± 22

Table 3 Elemental concentrations of Th, U and K in the investigated samples with 1σ-uncertainties

Rock type	Elemental concentration		
	U (ppm)	Th (ppm)	K (%)
Granite Schist 66	7.7 ± 0.2	64.0 ± 1.3	1.16 ± 0.06
Marble 68	1.4 ± 0.1	6.1 ± 0.7	0.44 ± 0.05
Phyllite 69	3.2 ± 0.1	23.3 ± 0.7	1.74 ± 0.07
Amphibolite 70	1.7 ± 0.1	9.3 ± 0.6	0.11 ± 0.01
Phyllite 71	3.5 ± 0.2	21.9 ± 0.9	1.33 ± 0.07
Graphite Slate 64	6.9 ± 0.2	14.0 ± 0.7	1.39 ± 0.07

Table 1 The activity concentrations of ^{238}U and ^{232}Th daughter products in the investigated samples (with 1σ-uncertainties)

Rock type	^{238}U series (Bq kg^{-1})			^{232}Th series (Bq kg^{-1})		
	^{226}Ra	^{214}Pb	^{214}Bi	^{228}Ac	^{212}Pb	"^{208}Tl"
Granite Schist 66	100 ± 4	87 ± 3	98 ± 4	295 ± 12	200 ± 4	284 ± 9
Marble 68	17 ± 2	17 ± 2	17 ± 2	26 ± 4	21 ± 2	25 ± 3
Phyllite 69	39 ± 3	43 ± 2	38 ± 3	98 ± 7	80 ± 3	106 ± 5
Amphibolite 70	23 ± 3	19 ± 2	22 ± 2	35 ± 5	33 ± 3	46 ± 4
Phyllite 71	41 ± 3	48 ± 2	40 ± 3	98 ± 8	83 ± 3	86 ± 5
Graphite Slate 64	90 ± 4	79 ± 3	88 ± 4	59 ± 6	46 ± 3	65 ± 5

"^{208}Tl" is the measured ^{208}Tl activity concentration divided by the branching ratio 0.362

Table 4 Calculated absorbed dose rates in air (1 m above ground) and annual effective dose rates outdoors and indoors (with the respective rock as building material)

Rock type	Absorbed dose rate (nGy h^{-1}) 1 m above ground	Annual effective dose (mSv $year^{-1}$) Outdoors	Annual effective dose (mSv $year^{-1}$) Indoors
Granite Schist 66	228	0.28	1.57
Marble 68	29	0.04	0.20
Phyllite 69	103	0.13	0.70
Amphibolite 70	35	0.04	0.24
Phyllite 71	95	0.12	0.66
Graphite Slate 64	93	0.11	0.63

showed numbers greater than 80 nGy h^{-1}. The world-wide population-weighted average is 59 nGy h^{-1} and the variability for measured absorbed dose rates in air (outdoors) is from 10 to 200 nGy h^{-1}. This means that 4 out of our 6 samples would be classified as delivering high dose rates in air. However, one has to keep in mind that we measured only isolated samples; to be able to give a comprehensive survey of the region direct dose rate measurements on the spot would be necessary.

By using an outdoor occupancy factor of 0.2 and a conversion coefficient of 0.7 Sv Gy^{-1} the annual effective dose (outdoors) was found to be between 0.04 and 0.28 mSv/a (world-wide average: 0.07 mSv/a). If earth and rock materials have been used as building materials, indoor exposure is inherently greater than the corresponding outdoor exposure. The indoor to outdoor ratio can go up to 2.3, with a population-weighted value of 1.4 [13]. As again data from direct indoor dose rate measurements are not available we used this factor 1.4 together with an indoor occupancy factor of 0.8 for the estimation of the indoor annual effective dose. Our results lie between 0.2 and 1.6 mSv/a (world-wide average: 0.41 mSv/a). We recommend that the investigated granite schist should not be used as a building material.

Conclusions

Gamma spectrometry provides a sensitive experimental tool for studying natural radioactivity and for determining elemental concentrations in various rock types. We investigated 6 samples from an area in southern Nepal and found specific activities in the range of 17–95 Bq kg^{-1} for ^{238}U, 24–260 Bq kg^{-1} for ^{232}Th and 32–541 Bq kg^{-1} for ^{40}K.

From these data we calculated the absorbed dose rates in air at a level of 1 m above ground and gave also an estimate of the annual effective dose to people living there assuming that they spend 20% of their time outdoors. Compared to UNSCEAR data collected over the whole world we found that 4 out of our 6 samples would be classified as delivering high dose rates in air. The highest annual effective dose outdoors is the fourfold of world-wide average of 0.07 mSv/a. Only speculative is the calculation of indoors annual effective doses, but we can at least conclude that the investigated granite schist should not be used as a building material.

To give a comprehensive survey of the region direct dose rate measurements on the spot would be necessary. Additionally the determination of natural radionuclides in drinking water (leached from the surrounding bedrock) from local wells is recommended as a significant part of human radiation exposure derives from radionuclide intake via ingestion of water.

Acknowledgments We thank Motee Lal Sharma (Department of Chemistry, Trichandra Campus, Tribhuvan University, Kathmandu, Nepal) for bringing us in contact and helping with the sample preparation.

References

1. Choppin G, Liljenzin JO, Rydberg J (2002) Radiochemistry and nuclear chemistry, 3rd edn. Butterworth–Heinemann, Woburn, MA
2. Tortzis M, Tsertos H, Christofides S, Christodoulides G (2003) J Environ Radioact 70:223
3. Tortzis M, Tsertos H, Christofides S, Christodoulides G (2003) Radiat Meas 37:221
4. Hamby DM, Tynybekev AK (2002) Environ Monit Assess 73(2):101
5. Papp Z, Dezso Z, Daroczy S (1997) J Radioanal Nucl Chem 222:171
6. Akhter P, Rahman K, Orfi SD, Ahmad N (2007) Food Chem Toxicol 45:272
7. Al-Masri MS, Amin Y, Hassan M, Ibrahim S, Khalili HS (2006) J Radioanal Nucl Chem 267(2):337
8. Navas A, Soto J, Machin J (2002) Appl Radiat Isot 57:579
9. Freitas AC, Alencar AS (2004) J Environ Radioact 75:211
10. Xinwei L, Lingqing W, Xiaodan J (2006) J Radioanal Nucl Chem 267(3):669
11. Al-Saleh FS, Al-Berzan B (2006) J Nucl Radiat Phys 2(1):25
12. Papastefanou C, Stoulos S, Manolopoulou M (2005) J Radioanal Nucl Chem 266(3):367
13. United Nations Scientific Committee on the Effects of Atomic Radiation (UNSCEAR) (2000) Sources and effects of ionizing radiation, vol I. United Nations, New York

14. Stöcklin J, Bhattarai KD (1977) Geology of the Kathmandu Area and Central Mahabharata Range, Nepal Himalaya. Report of Department of Mines and Geology, Government of Nepal/United Nations Development Program (UNDP), pp 86
15. Degerlier M, Karahan G, Orger G (2008) J Environ Radioact 99:1018
16. Beck HL (1972) Proceedings of the second int. symposium on the natural radiation environment, Canada, NF-720805 P2
17. United Nations Scientific Committee on the Effects of Atomic Radiation (UNSCEAR) (1993) Sources and effects of ionizing radiation, vol I. United Nations, New York